Thin Solid Films 517 (2008) 57–61

Contents lists available at ScienceDirect

Thin Solid Films

journal homepage: www.elsevier.com/locate/tsf

Growth and characterization of Ge nanostructures selectively grown on patterned Si

M.H. Cheng [a], W.X. Ni [a,*], G.L. Luo [a], S.C. Huang [a], J.J. Chang [b], C.Y. Lee [b]

[a] National Nano Device Laboratories, Hsinchu, Taiwan
[b] Department of Electronics Engineering, National Chiao Tung University, Hsinchu, Taiwan

ARTICLE INFO

Available online 24 August 2008

Keywords:
Self-assembly Ge nanostructures
Selectively epitaxy
Oxide-patterned substrate
Planar unpatterned substrate
Chemical vapor deposition
Strain degree
Electron beam lithography

ABSTRACT

By utilizing different distribution of strain fields around the edges of oxide, which are dominated by a series of sizes of oxide-patterned windows, long-range ordered self-assembly Ge nanostructures, such as nano-rings, nano-disks and nano-dots, were selectively grown by ultra high vacuum chemical vapor deposition (UHV-CVD) on Si (001) substrates. High-resolution double-crystal symmetrical $\omega/2\theta$ scans and two-dimensional reciprocal space mapping (2D-RSM) technologies employing the triple axis X-ray diffractometry have been used to evaluate the quality and strain status of as-deposited as well as in-situ annealed Ge nanostructures. Furthermore, we also compare the quality and strain status of Ge epilayers grown on planar unpatterned Si substrates. It was found that the quality of all Ge epitaxial structures is improved after in-situ annealing process and the quality of Ge nano-disk structures is better than that of Ge epilayers on planar unpatterned Si substrates, because oxide sidewalls are effective dislocation sinks. We also noted that the degree of relaxation for as-deposited Ge epilayers on planar unpatterned Si substrates is less than that for as-deposited Ge nano-disk structures. After in-situ annealing process, all Ge epitaxial structures are almost at full relaxation whatever Ge epitaxial structures grew on patterned or unpatterned Si substrates.

1. Introduction

Ge islands on Si substrates have attracted great attention for their potential nanodevice applications. The spontaneous formation of Ge islands on Si substrates is through transformation from layer-to-layer to 3-dimensional islands, which is so-called Stranski–Krastanov (SK) growth mode. However, for optimal optical and electronic applications, it is a big challenge concerning precise control of the size, position, and shape of Ge islands directly grown on Si substrates by SK growth mode. Although many effects and attempts have been made to overcome the difficulty, among these methods, selective epitaxial growth (SEG) on pre-patterned Si substrates has been considered to be a promising method to fabricate long-range ordered self-assembled Ge islands directly grown on Si substrates [1–5]. Because of combining lithography with high resolution such as electron beam lithography and self-assembled techniques could effectively make long-range ordering and homogeneity of Ge islands selectively grown on Si substrates, which has advantage of studying collective circumstances of long-range ordered self-assembled Ge islands on Si substrates in a run.

In particular, it was found that ordered Ge self-assembled quantum dots (SAQDs) nucleate around the edge of oxides when oxide windows (SiO_2) were used in selective epitaxial growth (SEG) on pre-patterned Si substrates. This characteristic was attributed to different expansion coefficient between Si and SiO_2 which make Si could be tensile strained on the periphery of the oxide edge, leading to the nucleation of Ge adatoms around the edges of oxide [6–8]. By utilizing this characteristic, we attempted to change distribution of strain fields around the edge of oxides, which are dominated by different sizes of oxide-patterned window, in order to fabricate long-range ordered self-assembly Ge nanostructures selectively grown on oxide-patterned Si substrates.

In addition, in heteroepitaxial growth system, misfit and threading dislocations arising from lattice and thermal expansion mismatch mainly affect the performance of heterostructure devices [9] and the mismatch also cause the change of strain relaxation status in epitaxial structures. There are many studies focused on assessments of strain relaxation status of epitaxial SiGe or Ge buffer layers grown on planar Si substrates with different growth conditions [10–12]. In particular, it was reported that the density of dislocations was reduced by limiting the lateral growth dimensions [13] and Vanamu et al. utilized this approach to produce high quality Ge heteroepitaxial layers on pre-patterned Si substrates [14].

In order to understand the difference of strain relaxation status between Ge epilayers grown on planar unpatterned Si substrates and long-range ordered Ge heteroepitaxial nanostructures selectively grown on oxide-patterned Si substrates, the high-resolution X-ray diffraction (HR-XRD) techniques employing the triple axis X-ray diffractometry have been used to evaluate the quality and strain relaxation status for both kinds of samples. Furthermore, it is well known that the thermal processing could lead to the interdiffusion of Ge out of epitaxially strained SiGe or Ge active layers and could reduce

* Corresponding author. No. 26, Prosperity Road 1, Science-based Industrial Park, Hsinchu 30078, Taiwan. Fax: +886 3 5722715.
E-mail address: wxni@mail.ndl.org.tw (W.X. Ni).

0040-6090/$ – see front matter © 2008 Published by Elsevier B.V.
doi:10.1016/j.tsf.2008.08.149

the mobility, resulting in degradation of strained-channel MOSFET (metal–oxide–semiconductor field effect transistor) [15]. Therefore, the influence of in-situ annealing process on the quality and strain relaxation status of these Ge epitaxial structures is also examined in this study.

2. Experiment

P-type (100)-oriented silicon wafers of a resistivity of 15–25 Ω cm with a 100-nm-thick thermal oxide (SiO_2) were used as substrates in this study. After coating DSE-1010 positive electron beam resist (DONGJIN Chemical Co., Led.) onto the thermal oxide, electron beam exposure was carried out by Leica E-beam Weprint 200 stepper and then was developed by 2.38% tetramethylammonium hydroxide (TMAH) solution. After developing, the oxide-patterned window was defined by oxide etcher (TEL, Te-5000) and the sizes of oxide-patterned window with partially anisotropic oxide walls varying from 240 nm to 690 nm were fabricated. The DSE-1010 positive resist was stripped away, and the samples was dipped in diluted HF for 30 s to remove a negative oxide on the bottom of exposed Si substrate before loading into a ultra high vacuum chemical vapor deposition (UHV-CVD) (ANELVA, SRE-12) chamber. After thermal prebake at 900 °C for 10 min, the Ge epilayers using germane as a source substance were grown at 430 °C with a growth rate 0.055 Å/s for 3 h, but this growth rate was estimated from the germanium growth on planar unpatterned Si substrates. Therefore, the real thickness of Ge epitaxial nanostructures was measured by cross-section transmission electron microscopy (TEM) (JEOL, JSM 6500-F), operating at 200 kV. We also prepared Ge epitaxial layers grown on planar unpatterned Si substrates with a growth rate 0.055 Å/s for 1.5 h in order to correspond to the similar thickness of Ge epitaxial nanostructures selectively grown on oxide-patterned Si substrates. Furthermore, these Ge epitaxial structures were in-situ annealed at 680 °C for 10 min at ultra high vacuum (10^{-9} torr).

A high-resolution PANalytical X'Pert Material Research Diffractometer equipped with a double-crystal and triple-axis mode was used to evaluate the quality and strain relaxation status of these Ge epitaxial structures. The double-crystal symmetrical $\omega/2\theta$ scans, where ω is the angle between incidence X-ray beams relative to the sample surface and 2θ is the diffraction angle, was performed by a high-resolution incident optics module with a small beam angular divergence (~30 arc-s), which results from two-bounce Ge (220) monochromator, and X-ray mirror. On the other hand, two-dimensional reciprocal space mapping (2D-RSM) technology was used to analyze the lattice parameters and strain relaxation status of Ge epitaxial structures in-detailed. 2D-RSM requiring a small 2θ acceptance angle was performed by a three-bounce Ge analyzer crystal (acceptance angle ~12 arc-s), which is so-called triple-axis mode. 2D-RSM is accomplished by scanning symmetric (004) and asymmetric (113) reciprocal lattice points, in which it consist of several coupled $\omega/2\theta$ scans for a range of incident angles $\omega \pm \Delta\omega$ as starting values. The detailed geometry of measurement conditioning could

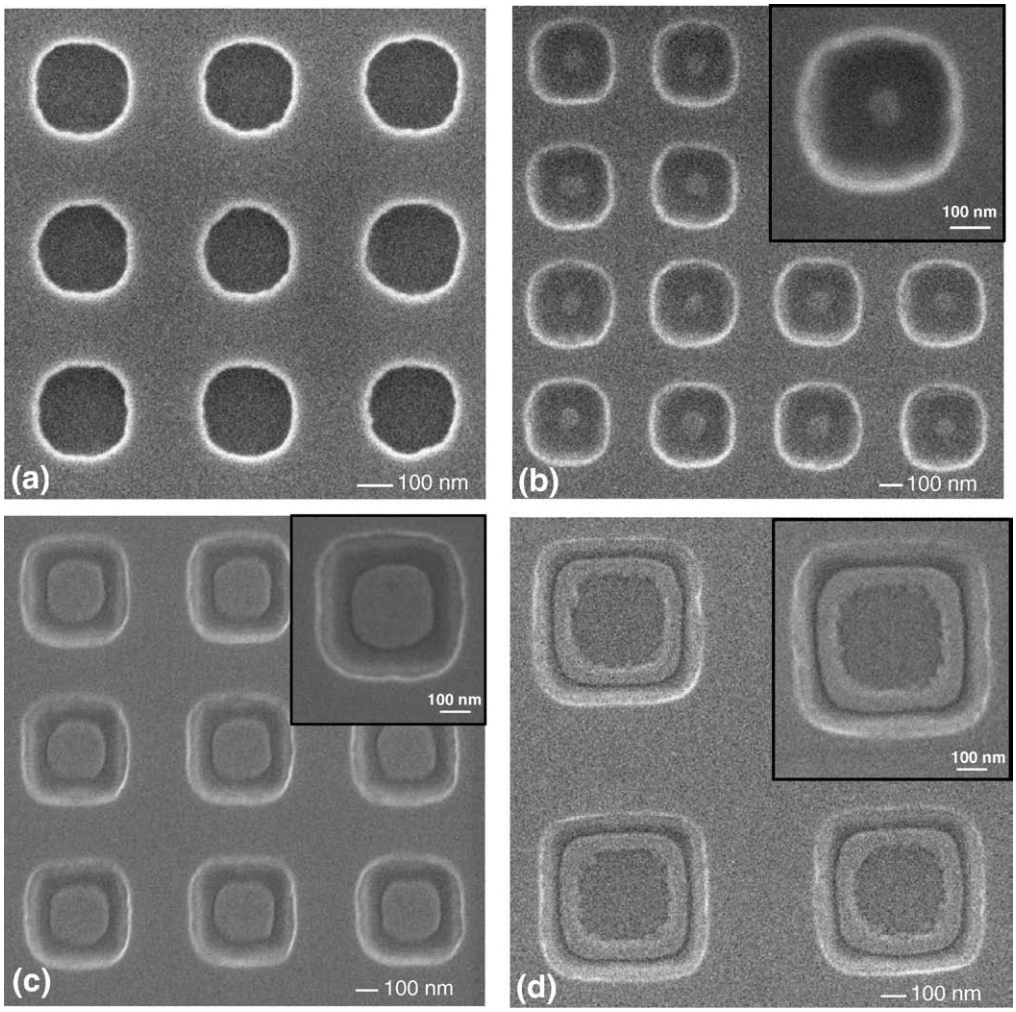

Fig. 1. SEM images of Ge epitaxial nanostructures grown on patterned Si substrates. (a) No Ge species grown on the window size 240 nm, (b) Ge nano-dot structures grown on the window size 320 nm, (c) Ge nano-disk structures grown on the window size 440 nm, (d) Ge nano-ring structures grown on the window size 690 nm.

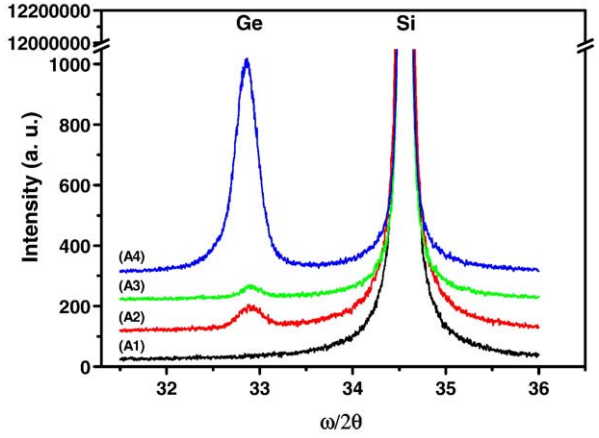

Fig. 2. High-resolution double-crystal symmetrical $\omega/2\theta$ scans of as-deposited Ge epitaxial structures. (A1) nano-dots, (A2) nano-disks, (A3) nano-rings, (A4) an as-deposited Ge epilayer grown on planar unpatterned Si substrates.

refer to Fewster's book [16]. After measuring 2D-RSM, the detailed lattice parameters of Ge epitaxial structures could be extracted. The lattice parameters include parallel relative lattice mismatch ($f_{//}$), perpendicular relative lattice mismatch ($f_{\perp}$), equivalent lattice mismatch (f) and the degree of relaxation (R) and each of lattice parameters can be expressed by using following equations:

$$f_{\perp} = \frac{\Delta a_{\perp}}{a(s)} = \frac{\Delta\left(\frac{1}{Q_{\perp}}\right)}{\frac{1}{Q(s)}} = \frac{Q_{\perp}(\mathscr{l}) - Q(s)}{Q_{\perp}(\mathscr{l})} \tag{1}$$

$$f_{//} = \frac{\Delta a_{//}}{a(s)} = \frac{\Delta\left(\frac{1}{Q_{//}}\right)}{\frac{1}{Q(s)}} = \frac{Q_{//}(\mathscr{l}) - Q(s)}{Q_{//}(\mathscr{l})}. \tag{2}$$

Where the indices $\mathscr{l}$ and s represent the layer and substrate, respectively. However, the degree of relaxation can be calculated by:

$$R = \frac{a_{//} - a(s)}{a_{\text{relaxed}} + a(a)} = \frac{f_{//}}{f} \tag{3}$$

$$f = (f_{\perp} - f_{//})\frac{1-\nu}{1+\nu} + f_{//} \tag{4}$$

Where f is the equivalent lattice mismatch based on the bulk elastic theory for a homogeneous deformation [17]. The detailed principles of 2D-RSM could refer to previous literature [18–20]. The surface morphology was performed by scanning electron microscopy (SEM) (JEOL, JSM 6500-F) and atomic force microscopy (VEECO, D-5000). The cross-section TEM samples were prepared by dual-beam focused ion beam (FEI, NOVA-200).

3. Results and discussion

A series of sizes of oxide-patterned window are prepared in order to fabricate different morphology of long-range ordered self-assembly Ge nanostructures selectively grown on Si substrates. We can observe that there is no Ge species grown into the oxide-patterned window when the size of oxide-patterned window is 240 nm, as shown in Fig. 1 (a), whereas the start of the nucleation appears at the window size 330 nm. This is possibly because the widow size of 240 nm is too small to diffuse Ge precursor molecules into the window. As the window sizes become wider, the morphology of long-range ordered self-assembly Ge nanostructures changes from nano-dot, nano-disk, and nano-ring structures as shown in Fig. 1(b), (c), and (d), respectively. The changes of Ge epitaxial structure morphology are attributed to the different distribution of strain fields around the edges of oxide, which are dominated in a series of sizes of oxide-patterned window. Since the expansion coefficient of Si is higher than that of SiO_2, leading to the higher tensile strain of Si near the edges of oxide, then this area could form diffusion sink sites. For example, the reason for the formation of unique Ge nano-ring structures is that the higher tensile strain of Si around the oxide-patterned edge makes the migration of Ge adatoms more easy to gather diffusion sink sites and gradually form growth of nano-ring structures to relax the system back toward equilibrium. The detailed mechanism can be found elsewhere [21].

Fig. 2 shows high-resolution double-crystal symmetrical $\omega/2\theta$ scans of as-deposited Ge nanostructures on oxide-patterned Si substrates which are named A1, A2, and A3 for Ge nano-dot, nano-disk, and nano-ring structures and an as-deposited Ge epilayer on a planar Si substrate which is named A4. From the diffraction spectrum, we can determine that the intensity of the sample A3 is weaker than that of sample A2 and this result is in agreement with our expectancy. Although the Ge nano-ring structures are grown on wider window sizes (690 nm) compared with that of Ge nano-disk structures (440 nm), Ge species nucleate around the edges of the oxide-patterned window for Ge nano-ring structures; therefore, the lack of complete Ge structure inside the oxide-patterned window reduce the intensity of diffraction compared with Ge nano-disk structures, which have the complete Ge structures inside each oxide-patterned window. Furthermore, in order to further study the complete Ge nano-disk structures inside each oxide-patterned window, three-dimension (3D)

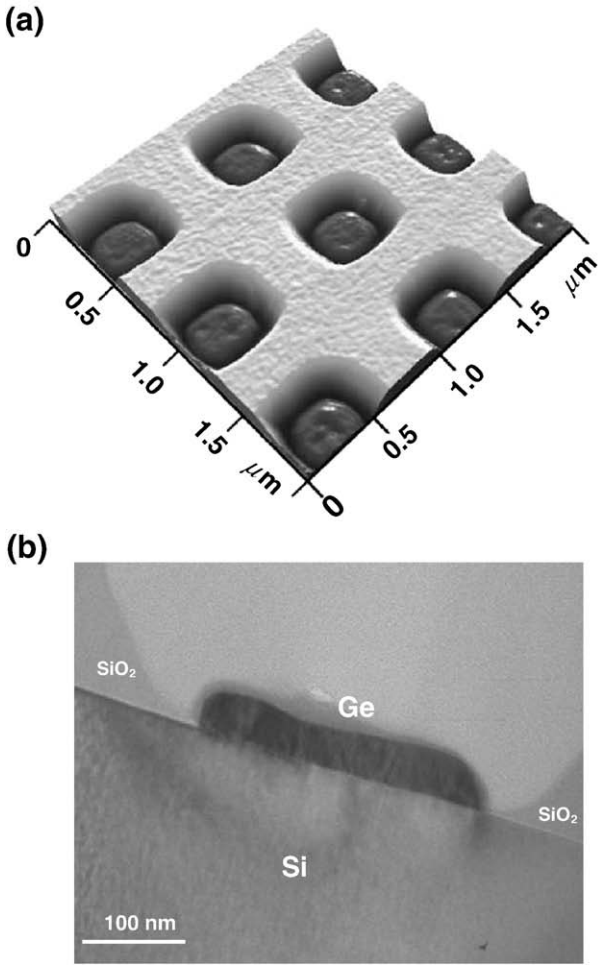

Fig. 3. (a) 3D AFM image of as-deposited Ge nano-disk structures grown on an oxide-patterned Si substrate, (b) a cross-section TEM image of a Ge nano-disk structure.

AFM and cross-section TEM were employed to analyze the complete and detailed Ge nano-disk structures.

Fig. 3(a) shows 3D AFM image of Ge nano-disk structures grown on an oxide-patterned Si substrate. It is clearly seen that each oxide-patterned window has a complete Ge structure inside, contributing to higher diffraction intensity than that of Ge nano-ring structures. Furthermore, a cross-section TEM image of a Ge nano-disk structure (in Fig. 3(b)) further reveals that the complete Ge nano-disk structure inside the window closely connects with the edges of partially anisotropic oxide wall, which has a deep slope of about 40° and we suppose that this feature could be also a significant factor to form diffusion sink sites around oxide-patterned edges. It is also noted that the thickness of Ge nano-disk is about 25 nm, which is thinner than that of Ge epilayers grown on unpatterned Si substrates at the same growth rate. This is possibly because selective epitaxial growth (SEG) on patterned Si substrates should consider the existence of patterns, which could be barriers when Ge precursor molecules attempted to diffuse into the patterned windows.

The influence of in-situ annealing on Ge epitaxial structures is also examined by high-resolution double-crystal symmetrical $\omega/2\theta$ scans, as shown in Fig. 4, which are named samples B1, B2, B3 and B4 with respect to samples A1, A2, A3 and A4 just after in-situ annealing process. It is evident that the quality of all Ge epitaxial structures is improved, resulting from the higher diffraction intensity and narrower full widths at half maximum (FWHMs) of all Ge epitaxial structures. However, we note that the FWHM of sample B2 (0.147°) is narrower than that of sample B4 (0.167°), which means that the quality of Ge nano-disk structures grown on oxide-patterned Si is better than that of the Ge epilayer grown on planar Si. The improved quality could be attributed to the mechanism of thermal-stress induced dislocation glide and annihilation and oxide sidewalls are effective dislocation sinks which reduce dislocations by gliding dislocations to dislocation sinks during in-situ annealing process. The similar observation was reported on a previous publication [22].

However, it is not an enough analysis to evaluate FWHM of all Ge epitaxial structures in double-crystal symmetrical $\omega/2\theta$ scans because it is well known that there are many factors, such as defects, finite thickness, strain, and mosaic effect, which cause the broadening of FWHM of epitaxial structures in double-crystal diffraction measurements. Therefore, in order to understand detailed strain relaxation status and quality of all Ge epitaxial structures, two-dimensional reciprocal space mapping (2D-RSM) technologies employing the triple axis X-ray diffractometry have been used to separate these effects and precisely evaluate the quality and strain relaxation status in all Ge epitaxial structures. Fig. 5(a) and (b) display 2D-RSM around (113) asymmetric reciprocal lattice points from samples A2 and A4. We can observe that the smaller elongation along $\omega/2\theta$ scan direction or ω scan direction for sample A2 as compared with sample A4, which implies the better quality for sample A2 than that of sample A4. This feature is consistent with previous report that the density of dislocations could be reduced by limiting the lateral growth dimensions [13]. On the other hand, the degree of relaxation in all Ge epitaxial structures are also extracted from 2D-RSM and the detailed lattice parameters of Ge epitaxial structures are tabulated in Table 1. It can be found that the degree of relaxation for as-deposited Ge epilayers on planar unpatterned Si substrates is less than that for as-deposited Ge nano-disk structures on patterned Si substrates. Moreover, after in-situ annealing process, all Ge epitaxial structures are

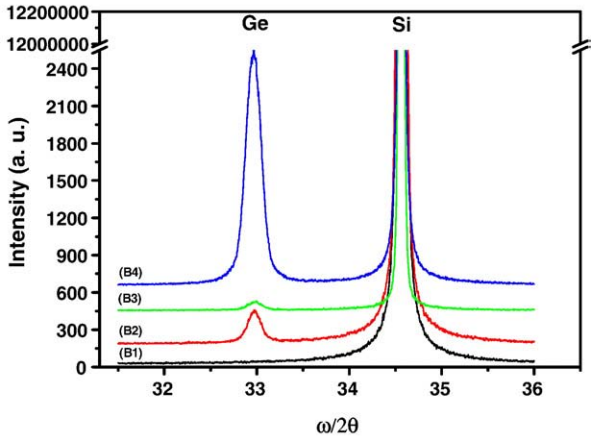

Fig. 4. High-resolution double-crystal symmetrical $\omega/2\theta$ scans of in-situ annealed Ge epitaxial structures. (B1) nano-dots, (B2) nano-disks, (B3) nano-rings, (B4) a in-situ annealed Ge epilayer grown on planar unpatterned Si substrates.

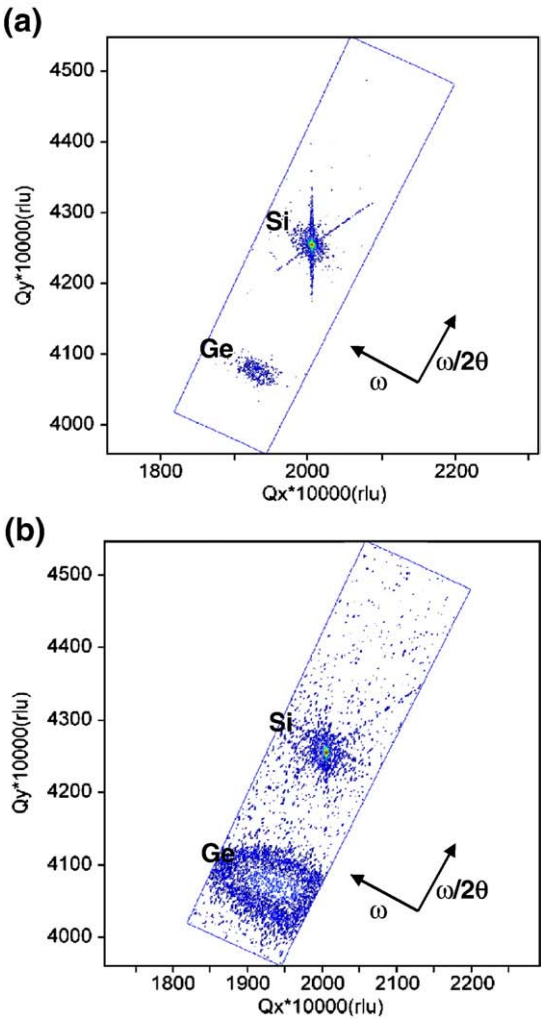

Fig. 5. (a) 2D-RSM around the asymmetric (113) reciprocal lattice points obtained from sample A2, (b) 2D-RSM around the asymmetric (113) reciprocal lattice points obtained from sample A4.

Table 1
Lattice parameters of different Ge epitaxial structures extracted from 2D-RSM

Sample	$f_{\perp}$ (%)	$f_{\parallel}$ (%)	f (%)	R (%)
Sample A2	4.59	3.75	4.23	89
Sample A4	4.52	3.11	3.91	80
Sample B2	4.26	3.84	3.92	98
Sample B3	4.06	4.34	4.18	103

$f_{\perp}$: perpendicular relative lattice mismatch, $f_{\parallel}$: parallel relative lattice mismatch, f: equivalent lattice mismatch, R: Relaxation=$f_{\parallel}/f$.

almost at full relaxation whatever Ge epitaxial structures grew on patterned or unpatterned Si substrates.

4. Conclusion

High-resolution double-crystal symmetrical $\omega/2\theta$ scans and two-dimensional reciprocal space mapping (2D-RSM) technologies employing the triple axis X-ray diffractometry were used to evaluate the quality and strain status of as-deposited and in-situ annealed Ge epitaxial structures grown on patterned or unpatterned Si substrates. The results indicate that the quality of all Ge epitaxial structures is improved; moreover, the quality of Ge nano-disk structures on patterned Si substrates is better than that of Ge epilayers on planar unpatterned Si substrates. It was found that the degree of relaxation for as-deposited Ge epilayers on planar unpatterned Si substrates is less than that for as-deposited Ge nano-disk structures on patterned Si substrates.

References

[1] T.I. Kamins, R.S. Williams, Appl. Phys. Lett. 71 (1997) 1201.
[2] Z. Zhong, A. Halilovic, T. Fromherz, F. Schaffler, G. Bauer, Appl. Phys. Lett. 82 (2003) 4779.
[3] Z. Zhong, G. Bauer, Appl. Phys. Lett. 84 (2004) 1922.
[4] J.T. Robinson, J.A. Liddle, A. Minor, V. Radmilovic, D.O. Yi, P.A. Greaney, K.N. Long, D.C. Chrzan, O.D. Dubon, Nano Lett. 5 (2005) 2070.
[5] T.S. Yoon, Z. Zhao, J. Liu, Y.H. Xie, D.Y. Ryu, T.P. Russell, H.M. Kim, K.B. Kim, Appl. Phys. Lett. 89 (2006) 063107.
[6] T. Stoica, L. Vescan, E. Sutter, J. Appl. Phys. 95 (2004) 7077.
[7] L. Vescan, T. Stoica, B. Hollander, A. Nassiopoulou, A. Olzierski, I. Raptis, E. Sutter, Appl. Phys. Lett. 82 (2003) 3517.
[8] E.S. Kim, N. Usami, Y. Shiraki, Appl. Phys. Lett. 72 (1998) 1617.
[9] R.M. Sieg, J.A. Carlin, J.J. Boeckl, S.A. Ringel, M.T. Currie, S.M. Ting, T.A. Langdo, G. Taraschi, E.A. Fitzgerald, B.M. Keyes, Appl. Phys. Lett. 73 (1998) 31111.
[10] M.Y.A. Yousif, O. Nur, M. Willander, C.J. Patel, C. Hernandez, Y. Campidelli, D. Bensahel, R.N. Kyutt, Solid-State Electron. 45 (2001) 1869.
[11] T. Myrberg, A.P. Jacob, O. Nur, M. Friesel, M. Willander, C.J. Patel, Y. Campidelli, C. Hernandez, O. Kermarrec, D. Bensahel, J. Mater. Sci., Mater. Electron. 15 (2004) 411.
[12] D.O. Shin, M.R. Sardela Jr, S.H. Ban, N.E. Lee, K.H. Shim, Appl. Surf. Sci. 237 (2004) 139.
[13] J.W. Mathews, S. Mader, T.B. Light, J. Appl. Phys. 41 (1970) 3800.
[14] G. Vanamu, A.K. Datye, S.H. Zaidi, J. Vac. Sci. Technol., B 23 (2005) 1622.
[15] M.L. Lee, E.A. Fitzgerald, M.T. Bulsara, M.T. Currie, A. Lochtefeld, J. Appl. Phys. 97 (2005) 011101.
[16] P.F. Fewster, X-ray Scattering from Semiconductors, Imperial College Press, London, 2000.
[17] J. Hornstra, W.J. Bartels, J. Cryst. Growth 44 (1978) 513.
[18] W.X. Ni, K. Lyutovich, J. Alami, C. Tengstedt, M. Bauer, E. Kasper, J. Cryst. Growth 227–228 (2001) 756.
[19] E. Koppensteiner, G. Bauer, H. Kibbel, E. Kasper, J. Appl. Phys. 76 (1994) 3489.
[20] G. Bauer, J. Li, E. Koppensteiner, J. Cryst. Growth 157 (1995) 61.
[21] M.H. Cheng, G.L. Luo, W.X. Ni, in press.
[22] H.C. Luan, D.R. Lim, K.K. Lee, K.M. Chen, J.G. Sandland, K. Wada, L.C. Kimerling, Appl. Phys. Lett. 75 (1999) 2909.